Theoretical and Experimental Studies of the Reaction of OH with Isoprene

Philip S. Stevens*,† and Eric Seymour

School of Public and Environmental Affairs, Indiana University, Bloomington, Indiana 47405

Zhuangjie Li*,‡

Department of Atmospheric Sciences, University of Illinois, Urbana, Illinois 61801

Received: October 11, 1999; In Final Form: March 28, 2000

The structure and energetics for the reaction of OH + isoprene → adduct have been examined using ab initio molecular orbital methods. The structure of each HO−isoprene adduct was optimized using Becke's three-parameter hybrid method employing the LYP correction functional (B3LYP) with the 6-31G** basis set, and using Møller−Plesset correlation energy correction truncated at second-order (MP2) with both the 6-31G** and the 6-311G** basis sets. Single-point energy calculations using fourth-order Møller−Plesset perturbation theory including single, double, triple, and quadruple excitations, as well as spin projection (PMP4(SDTQ)) with the 6-311G** basis set, were carried at these optimized geometries. The single-point energy was further corrected with zero-point energy (ZPE) to assess the stability of the OH−isoprene adducts. At the PMP4-(SDTQ)/6-311G**//MP2/6-311G** + ΔZPE level of theory addition of OH to the 1 and 4 carbons of isoprene produces adducts which are 37.9 and 35.4 kcal mol^{-1} (respectively) more stable than the OH and isoprene reactants, while addition of OH to the 2 and 3 carbons results in adducts which are 25.6 and 24.2 kcal mol^{-1} more stable than the reactants. Experimental detection of the products from the OH + isoprene reaction using a discharge-flow system coupled with a mass spectrometer shows evidence for the production of all four possible adducts. These results suggest that each adduct is formed with nonnegligible yields, allowing each to participate in subsequent steps in the OH-initiated oxidation of isoprene.

Introduction

The mechanism of the OH-initiated oxidation of isoprene (2-methyl-1,3-butadiene) has received a substantial amount of attention in atmospheric chemistry.[1−20] Isoprene is one of the dominant hydrocarbons emitted into the atmosphere by vegetation, and can contribute to urban and regional production of ozone in the troposphere because of its high reactivity with the hydroxyl radical (OH). A detailed knowledge of the mechanism of the oxidation of isoprene is essential in order to simulate accurately urban and regional air quality.

The OH-initiated oxidation of isoprene emissions in the atmosphere proceeds primarily through addition of OH to the carbon−carbon double bonds, leading to the production of four hydroxyalkyl radicals (Figure 1). Addition of OH to the 1 or 4 carbon of isoprene results in the formation of allylic radicals with the unpaired electron delocalized over two radical centers. Each of these radicals leads to the formation of two different peroxy radicals depending on the position of the O_2 addition. As a result, the OH-initiated oxidation of isoprene leads to the formation of six different peroxy radicals. Under polluted conditions characterized by high NO concentrations, these peroxy radicals are assumed to quickly react with NO to form hydroperoxy radicals (HO_2), NO_2, ozone, and subsequent oxidation products (reactions 1−5 for example):

$$OH + CH_2{=}C(CH_3)CH{=}CH_2 + M \rightarrow HOCH_2C(CH_3)CH{=}CH_2 + M \quad (1a)$$

$$HOCH_2C(CH_3)CH{=}CH_2 + O_2 + M \rightarrow HOCH_2C(O_2)(CH_3)CH{=}CH_2 + M \quad (1b)$$

$$HOCH_2C(O_2)(CH_3)CH{=}CH_2 + NO \rightarrow HOCH_2C(O)(CH_3)CH{=}CH_2 + NO_2 \quad (2)$$

$$HOCH_2C(O)(CH_3)CH{=}CH_2 \rightarrow CH_2OH + CH_3C(O)CH{=}CH_2 \quad (3a)$$

$$CH_2OH + O_2 \rightarrow HCHO + HO_2 \quad (3b)$$

$$HO_2 + NO \rightarrow OH + NO_2 \quad (4)$$

$$NO_2 + h\nu \rightarrow O + NO \quad (5a)$$

$$O + O_2 + M \rightarrow O_3 + M \quad (5b)$$

Reactions of each peroxy radical with NO and O_2 likely results in the production of methyl vinyl ketone from OH addition to the 1 and 2 carbon of isoprene, methacrolein from OH addition to the 3 and 4 position, and carbonyl production from addition to the 1 and 4 positions (Figure 1).[1,2] It has been assumed that OH favors addition to the trisubstituted bond in isoprene (position 1 and 2),[1,3,4] while there is experimental evidence from the OH + methyl vinyl ketone reaction that suggests that OH addition to the terminal (1 and 4) carbons is favored 70% of the time.[5]

There have been several experimental measurements of the kinetics and mechanism of the OH-initiated oxidation of isoprene. These include absolute[6,7] and relative[3,8−11] rate constant measurements of the OH + isoprene reaction, and product

† E-mail: pstevens@indiana.edu. Fax: (812) 855-7802.
‡ E-mail: zli@atmos.uiuc.edu. Fax: (217) 244-4393.

10.1021/jp993612i CCC: $19.00
Published on Web 05/17/2000

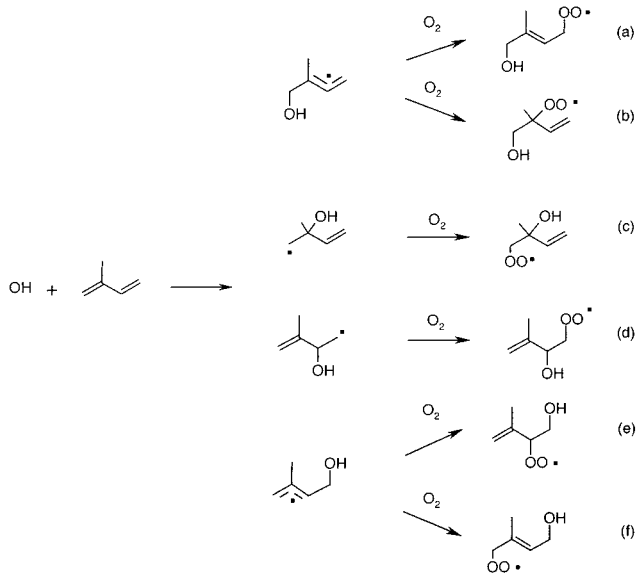

Figure 1. Schematic mechanism of the OH-initiated oxidation of isoprene.

studies of the oxidation mechanism in the presence of NO_x.[12−19] The product studies have identified and quantified the primary products of the OH-initiated oxidation of isoprene to be methyl vinyl ketone, methacrolein, and formaldehyde, with yields of approximately 0.32 and 0.23 for methyl vinyl ketone and methacrolein, respectively.[19] However, there is still uncertainty associated with the overall mechanism of the OH-initiated oxidation of isoprene, as approximately 40% of the total carbon oxidized in the mechanism has not been quantified, although organic nitrates and hydroxycarbonyls have been identified in recent studies.[17,18,20] In addition, recent ambient measurements of methacrolein and methyl vinyl ketone in the remote troposphere were much lower than predicted, suggesting either a more efficient loss process for these molecules or a less efficient formation process.[21]

Despite the substantial and growing experimental database on the OH-initiated oxidation of isoprene, there have been few theoretical studies of this and other OH + alkene reactions with the exception of the reactions of OH with ethylene and propene.[22,23] It is important to characterize the species from the initial step of the isoprene oxidation in order to better understand the subsequent oxidation process of isoprene in the atmosphere. This paper presents the results of ab initio calculations on the individual hydroxyalkyl radical adducts formed from the OH + isoprene reaction. The primary goal of this paper is to examine the relative stability of each OH−isoprene adduct to determine theoretically the product channels that are the most energetically stable. These theoretical results are used in unimolecular rate theory to predict the rate constant for the OH + isoprene reaction at the low-pressure limit and compared to experimental detection of the products from the OH + isoprene reaction.

Computational Methods

The computations were conducted using the HyperChem[24] and Gaussian 98 programs.[25] Initial geometry optimizations for the species involved in the OH + isoprene → adduct reaction were performed at the Hartree−Fock (HF) level of theory using the 6-31G** basis set. The geometry of each adduct was further optimized using Becke's three-parameter hybrid method employing the LYP correction functional (B3LYP) with 6-31G** basis set and using second-order Møller−Plesset perturbation theory (MP2) in conjunction with both the 6-31G** and 6-311G** basis sets. Frequencies for both reactants and products were calculated at B3LYP/6-31G** level of theory. Single-point energy calculations at the MP2/6-311G** optimized geometries were calculated using fourth-order Møller−Plesset perturbation theory including single, double, triple, and quadruple excitations, and with spin projection (PMP4SDTQ) in conjunction with the 6-311G** basis set.

Experimental Methods

The products of the OH + isoprene reaction were measured and identified at a pressure of 1−10 Torr using a discharge flow system coupled with a mass spectrometer (DF/MS). The details of the experimental system are described elsewhere.[26] OH radicals were produced using the $F + H_2O$ reaction from a microwave discharge of trace F_2 in helium through a movable injector. OH radicals were detected using resonance fluorescence techniques. Isoprene (Aldrich, 99%) was degassed by several freeze−pump−thaw cycles before use and was detected with the mass spectrometer at $m/e = 68$. The absolute concentration of isoprene detected by the mass spectrometer was calibrated by introducing measured flows of a known dilute isoprene mixture into the flow system. The dilute mixtures were prepared by vacuum distilling known aliquots of isoprene into a bulb and then diluting with helium. Concentrations of isoprene and products were measured by the mass spectrometer by continuous sampling at the downstream end of the flow tube through a two-stage differentially pumped beam inlet system.

Results and Discussion

Ab Initio Calculations. Figure 2 summarizes the optimized geometry calculated at both the MP2/6-31G** and MP2/6-311G** levels of theory for each of the HO−isoprene adducts. The geometry optimized at B3LYP/6-31G** level of theory for each adduct is consistent with that optimized at MP2/6-31G** level of theory with a difference of less than 1% in all bond lengths and bond angles. The calculated C−C bond lengths for isoprene are in excellent agreement with experimentally determined values (C═C 1.340 Å, C−C 1.463 Å, $C-C_{methyl}$ 1.512 Å).[27] Although there are two configurations (cis and trans) for the isoprene molecule, the trans isomer is more stable than the cis isomer.[27] Hence the OH addition to the trans isoprene has been the primary focus of the present investigation. To check that the trans structure of the carbon backbone of the adducts was the most energetically stable isomer, we optimized a cis configuration of adduct 2. It was found that at the MP2/6-311G** level of theory, the cis configuration was only 1.5 kcal mol^{-1} less stable than the corresponding trans structure, suggesting that the difference between the cis and trans forms of the adducts is relatively small.

Addition of OH to any of the four positions does not substantially affect the trans structure of the isoprene carbon backbone (the CCC bond angles) or the structure of the methyl group. However, comparing the structures of the adducts to isoprene shows that addition of OH to each site changes the C−C bonding characteristics of the system. Addition of OH to the 1 carbon of isoprene (adduct 1) leads to a lengthening of the C−C bond between carbons 1 and 2 by 0.151 Å relative to isoprene, reflecting an increased σ character of the C−C bond as electron density in the Π bond is transferred to the C−O bond. A similar lengthening of the C−C bond between carbons 1 and 2 (0.150 Å) is also predicted upon addition of OH to the 2 carbon of isoprene (adduct 2). Addition of OH to the number

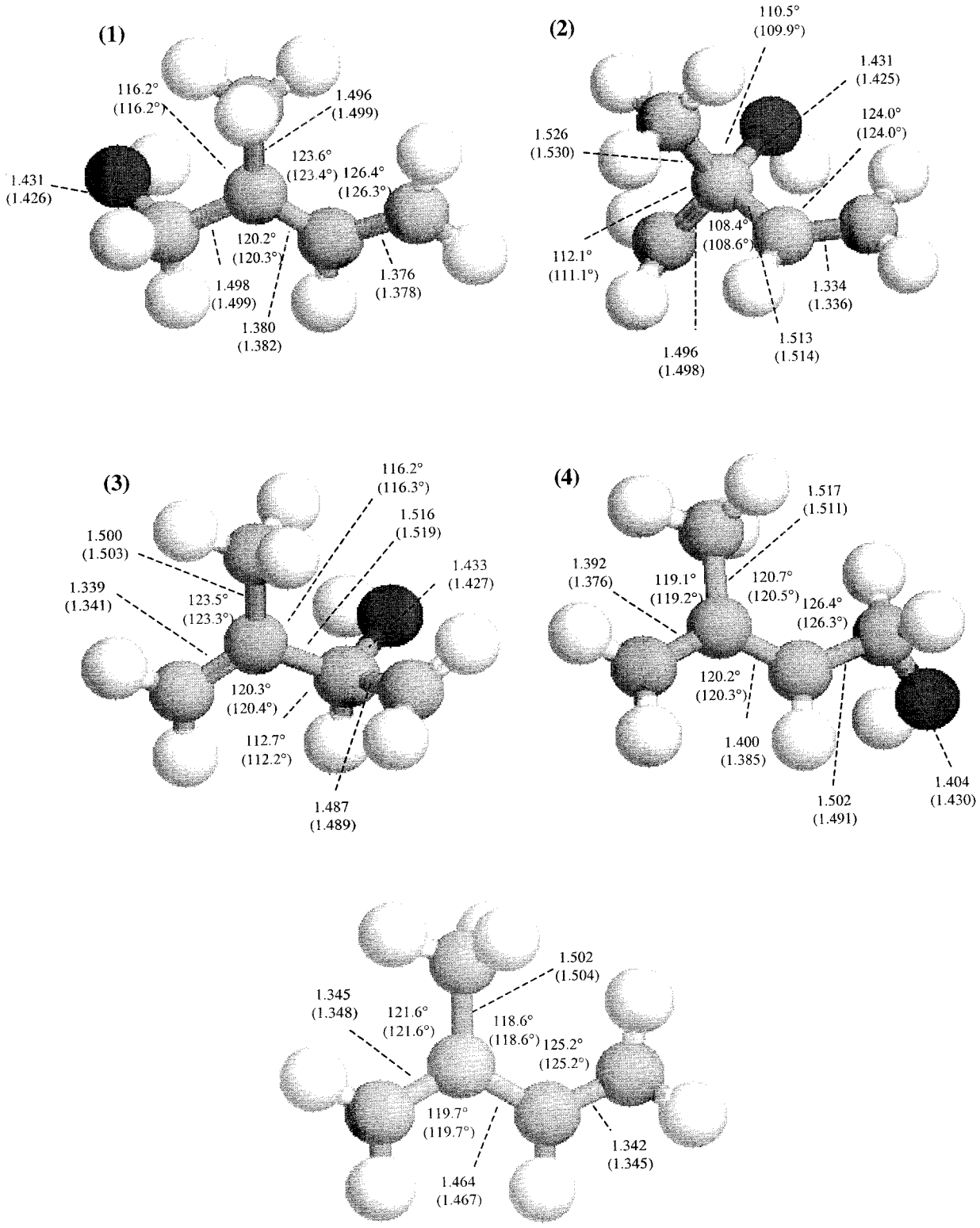

Figure 2. Optimized geometries at the MP2/6-31G** level of theory for isoprene and the HO−isoprene adducts. C−C and C−O bond lengths are in angstroms, and C−C−C angles are in degrees. Values in parentheses are computed at the MP2/6-311G** level of theory.

3 and number 4 carbon results in a lengthening of the C−C bond between carbons 3 and 4 by 0.144 and 0.146 Å, respectively. This again reflects the increased σ character of the bond resulting from the transfer of electron density from the Π bond to the newly formed C−O bond.

The C−C single bond between carbon 2 and 3 in isoprene (1.467 Å) is lengthened by 0.047 and 0.052 Å, respectively, upon OH addition in adducts 2 and 3. However, the length of the terminal C−C double bond between carbons 3 and 4 in adduct 2 (1.336 Å), and between carbons 1 and 2 in adduct 3 (1.341 Å), are comparable to the corresponding bonds in isoprene (1.348 and 1.345 Å respectively), reflecting significant Π bonding character for these C−C bonds. This suggests that the bonding characteristics of the terminal carbon pair in adducts 2 and 3 not involved in the OH addition is not significantly affected upon adduct formation, and that the unpaired electron in adducts 2 and 3 is localized on the terminal carbon adjacent to the point of addition.

TABLE 1: Total Energy (in hartrees) and Spin Eigenvalues for the OH + Isoprene → Adduct Reaction

species	HF/6-31**	MP2/6-3**	MP2/6-311G**	MP4(SDTQ)[a]	PMP4(SDTQ)[a]	S^2(MP2)	B3LYP/6-31G**	S^2(B3LYP)
OH	−75.388 33	−75.534 38	−75.591 40	−75.607 14	−75.607 96	0.755	−75.721 75	0.752
isoprene	−193.970 92	−194.683 63	−194.816 63	−194.904 66	−194.904 66	0	−195.322 54	0
adduct 1	−269.409 51	−270.277 92	−270.467 50	−270.568 99	−270.579 09	0.945	−271.120 27	0.778
adduct 2	−269.380 65	−270.266 13	−270.456 66	−270.555 99	−270.557 25	0.763	−271.091 67	0.754
adduct 3	−269.382 49	−270.264 52	−270.454 87	−270.553 92	−270.555 18	0.750	−271.092 35	0.754
adduct 4	−269.406 45	−270.273 33	−270.462 94	−270.564 59	−270.574 94	0.952	−271.115 95	0.780

[a] Single-point calculation with 6-311G** basis set using the geometry optimized at MP2/6-311G** level.

TABLE 2: Calculated Frequencies (cm^{-1}) and Zero-Point Energy at the B3LYP/6-31G Level of Theory for the OH + Isoprene → Adduct Reaction[a]**

species	frequencies (cm^{-1})	experiment (cm^{-1})[b]	ZPE (kcal mol^{-1})
OH	3694	3735	5.3
isoprene	3249, 3242, 3167, 3157, 3150, 3133, 3092, 3039, 1720, 1670, 1516, 1495, 1471, 1443, 1423, 1339, 1332, 1095, 1076, 1035, 1016, 968, 930, 923, 796, 789, 645, 535, 429, 408, 278, 206, 164	3097, 3092, 3020, 2988, 2978, 2956, 2928, 2910, 1638, 1603, 1466, 1425, 1422, 1414, 1388, 1303, 1291, 1069, 1034, 1012, 990, 953, 903, 891, 780, 755, 622, 523, 412, 401, 288, 199, 153	71.4
adduct 1	3797, 3262, 3171, 3132, 3132, 3091, 3048, 3014, 2999, 1542, 1514, 1508, 1503, 1469, 1428, 1411, 1390, 1349, 1255, 1238, 1190, 1061, 1040, 1030*, 993, 979, 933, 786, 782, 605, 550, 459, 392, 342, 292, 277, 191, 101, 70		80.5
adduct 2	3788, 3271, 3250, 3166, 3159, 3146, 3138, 3134, 3051, 1723, 1504, 1496, 1462, 1444, 1402, 1336, 1321, 1256, 1201, 1047, 1041*, 1030, 990, 959, 954, 890, 741, 703, 579, 528, 435, 417, 379, 320, 302, 287, 248, 126, 117		79.1
adduct 3	3807, 3922, 3228, 3175, 3146, 3134, 3101, 3042, 2938, 1724, 1511, 1486, 1461, 1459, 1415, 1391, 1320, 1292, 1241, 1115*, 1075, 1063, 1027, 970, 932, 893, 801, 749, 585, 561, 461, 421, 363, 350, 265, 226, 173, 105, 77		79.2
adduct 4	3801, 3255, 3164, 3158, 3132, 3102, 3046, 3036, 3004, 1536, 1515, 1511, 1498, 1476, 1433, 1409, 1388, 1356, 1279, 1192, 1144, 1060, 1046*, 1033, 1001, 927, 840, 796, 743, 569, 517, 492, 466, 376, 353, 237, 145, 135, 58		80.4

[a] An asterisk (*) indicates vibration with identifiable CO stretching component. [b] Experimental values from refs 27 and 28.

Unlike adducts 2 and 3, the C−C bond length between carbon 2 and 3 for adducts 1 and 4 (1.382 and 1.385 Å respectively) is shorter than that in isoprene, reflecting significant Π bonding character. In addition, the C−C double bond between carbons 3 and 4 in adduct 1 (1.378 Å) and between carbons 1 and 2 in adduct 4 (1.376 Å) are slightly larger than the corresponding bonds in isoprene, but similar to the bond length between carbons 2 and 3 of both adducts. These bond lengths are between the typical bond lengths for a σ bond and a Π bond and are consistent with significant Π bonding character between the terminal three carbons in adducts 1 and 4. This strongly suggests that the unpaired electron resulting from addition of OH to the terminal carbons is indeed delocalized in a resonance structure between the three terminal carbons, consistent with the allylic nature of these radicals.

The total energy along with the spin eigenvalues (S^2) associated with the optimized geometries for OH, isoprene, and each HO−isoprene adduct is listed in Table 1. Contamination of the unrestricted Hartree−Fock wave function from higher spin states is minimal for OH and adducts 2 and 3, as the expected value for S^2 for each of these species is close to the exact value of 0.750 for a pure doublet. However, the calculated values of S^2 for adducts 1 and 4 (0.945 and 0.952, respectively) at the MP2 level of theory show significant spin contamination. The spin contamination does not seem to significantly affect either geometry or frequencies of adducts 1 and 4 since these parameters are found to be consistent with that calculated at B3LYP/6-31G** level of theory, in which the values of S^2 are 0.778 and 0.780, respectively. The values of S^2 calculated after spin projection for adducts 1 and 4 were 0.757 and 0.758, suggesting that spin contamination of these wave functions is essentially removed after the spin projection.

Frequencies for all reactants and adducts were computed at both MP2/6-311G** and B3LYP/6-31G** levels of theory. While there was no substantial difference in the calculated frequencies at these levels of theory, it was found that the frequencies computed at B3LYP/6-31G** level of theory are in better agreement with the available experimental values for both OH and isoprene. Thus, we choose to use frequencies calculated at the B3LYP/6-31G** level for zero-point energy (ZPE) computation. Table 2 lists the calculated vibrational frequencies and zero-point energy at the B3LYP/6-31G** level of theory for OH, isoprene, and each adduct. The absence of any imaginary frequencies confirms that the optimized geometry for each adduct is a local minimum on the potential energy surface. At this level of theory, the calculated frequencies for OH and isoprene are within 10% of the experimental values.[27,28]

Our calculated results show that the vibrations within each HO−isoprene adduct are highly coupled with each other. This makes frequency assignments of the individual modes difficult.

TABLE 3: Relative Energetics (in kcal mol^{-1}) of the OH + Isoprene → Adduct Reaction

level of theory	adduct 1	adduct 2	adduct 3	adduct 4
HF/6-31G**	−31.5	−13.4	−14.6	−29.6
MP2/6-31G**	−37.6	−30.2	−29.2	−34.7
MP2/6-311G**	−37.3	−30.5	−29.4	−34.3
MP4(SDTQ)[a]	−35.9	−27.7	−26.4	−33.1
PMP4(SDTQ)[a]	−41.7	−28.0	−26.7	−39.1
B3LYP/6-31G**	−47.7	−29.7	−30.2	−45.0
ΔZPE	3.8	2.4	2.5	3.7
PMP4 w/ΔZPE[a]	−37.9	−25.6	−24.2	−35.4

[a] Single-point calculation with 6-311G** basis set using the geometry optimized at MP2/6-311G** level.

The vibration with a dominant C−O stretching component in each adduct is identified and labeled in Table 2. The C−O stretching frequency of the HO−isoprene adducts are predicted to be 1030−1115 cm^{-1}, a frequency range comparable to the typical C−O stretching for alcohol compounds such as CH_3OH (1034 cm^{-1} for CH_3OH).[29] Note that this vibrational mode is highly coupled to other motions in each adduct, which explains why the OH + isoprene reaction has reached its high-pressure limit at pressures as low as 2 Torr.[7] The highly coupled nature of these vibrations allows the critical energy resulting from the OH addition to be easily distributed across a number of vibrational modes of the adduct, which quickly stablilizes the energized adduct without many third-body collisions. Finally, it can be seen from Table 2 that the ZPE for each adduct is very similar.

Table 3 lists the relative energetics computed at each level of theory for the OH + isoprene reaction. Although calculations at both B3LYP and the PMP4(SDTQ)/6-311G**//MP2/6-311G** levels predict a exothermic process for the addition of OH to isoprene, we choose to use the PMP4(SDTQ)/6-311G**//MP2/6-311G** result for the best estimate of the thermodynamic properties of the OH + isoprene system since the B3LYP method uses semiempirical coefficients.[30] At the PMP4(SDTQ)/6-311G**//MP2/6-311G** + ΔZPE level of theory, adduct 1 is predicted to be the most stable among the four OH−isoprene complexes examined, with a calculated stability of −37.9 kcal mol^{-1} relative to the reactants. Adduct 4 is slightly less stable than adduct 1 (−35.4 kcal mol^{-1}), while adducts 2 and 3 (−25.6 and −24.2 kcal mol^{-1}) are approximately 13 kcal mol^{-1} less stable than adduct 1. This order of stability (adducts 1, 4, 2, 3) is not dependent on the level of theories applied in this study except at the HF and the B3LYP level, where the relative stabilities of adducts 2 and 3 are reversed. This implies that electron correlation is important in determining the absolute stability of the HO−isoprene adducts. Spin projection is also important in evaluating the stability of each complex, especially for adducts 1 and 4 due to a high level of spin contamination involved in their wave functions. Our best predicted energetic order of the both reactants and adducts for the OH + isoprene reaction is summarized in Table 3.

The relative stability of the adducts is not surprising considering the ability of adducts 1 and 4 to delocalize the electron density associated with the unpaired electron resulting from the radical addition. This delocalization is evident from the Π bonding character of the C_3-C_4 and C_2-C_3 bond lengths in adduct 1, and the C_1-C_2 and C_2-C_3 bond lengths in adduct 4. Thus, the increased stability of adducts 1 and 4 relative to adducts 2 and 3 is due to allylic resonance of the unpaired electron. Steric effects due to the methyl group do not seem to affect the relative stability of each adduct, as addition of OH to the 1 position is more stable than addition to the 4 position, and addition to the 2 position is more stable than addition to the 3 position.

Calculation of the Low-Pressure Limiting Rate Constant. To test whether the calculated stability of the adducts is consistent with experimental measurements, the results of these calculations were used to estimate the low-pressure limiting rate constants for the OH + isoprene → adducts reaction. At the low-pressure limit, the overall rate constant is limited by the rate of intermolecular energy transfer, which is dependent on the relative stability of the adducts.[31] The theoretical results were used in simplified equations based on RRKM theory to estimate the second-order rate constant for the unimolecular dissociation of the OH−isoprene adducts,[31−34] and the resulting rate constants were then used to estimate the reverse third-order association rate constant through the equilibrium constant for the OH + isoprene reaction, assuming that the barrier to formation of the adducts is negligible. This is not an unreasonable assumption based on the observed negative temperature dependence of the rate constant for this reaction.[6−8] Ab initio calculations of the transition state for the OH + propene reaction also reveal a negligible barrier for OH addition.[23] The resulting estimated OH + isoprene association rate constants were then compared to recent experimental measurements of the pressure and temperatue dependence of the OH + isoprene reaction at the low-pressure limit.

The strong collision dissociation rate constant at the low-pressure limit can be expressed as[32−34]

$$k_{\mathrm{diss}}^{\mathrm{sc}} = Z_{\mathrm{LJ}} \frac{\rho(E_0)RT}{Q_{\mathrm{vib}}} \exp\left(\frac{-E_0}{RT}\right) F_{\mathrm{E}} F_{\mathrm{anh}} F_{\mathrm{rot}} F_{\mathrm{corr}} \qquad (6)$$

where Z_{LJ} is the Lennard-Jones collision frequency, $\rho(E_0)$ is the density of states at the critical energy E_0, Q_{vib} is the vibrational partition function, and F_{E}, F_{anh}, and F_{rot} are correction terms for the energy dependence of the density of states, anharmonicity, and rotation. F_{corr} is a correction factor to account for coupling between the various degrees of freedom, and is assumed to be unity, which neglects the coupling between various vibrational and rotational degrees of freedom.[32] R is the ideal gas constant and T is the temperature in kelvin. The strong collision association rate constant can then be obtained from the calculated equilibrium constant:

$$k_{\mathrm{rec}}^{\mathrm{sc}} = \frac{k_{\mathrm{diss}}^{\mathrm{sc}}}{K_{\mathrm{eq}}} \qquad (7)$$

The strong collision association rate constant represents an upper limit to the observed rate constant and is multiplied by a collisional deactivation efficiency β_{c} to obtain the weak collision rate constant, $k_{\mathrm{rec}}^{\mathrm{wc}}$, which can be compared to experiment.[33,34]

The second-order rate of dissociation of the OH−isoprene adducts at low pressure will depend on the rate of energization of the adducts above the dissociation threshold, E_0. For these calculations, the relative stabilization energy of each adduct was used for E_0, as the barrier to dissociation is probably negligible. Z_{LJ} was calculated following Troe[32] and is given by

$$Z_{\mathrm{LJ}} = 8.09 \times 10^{-10}\ \mathrm{cm^3\ molecule^{-1}\ s^{-1}} \times \sqrt{\left(\frac{T}{1000\ \mathrm{K}}\right)\left(\frac{20\ \mathrm{g\ mol^{-1}}}{\mu_{\mathrm{AM}}}\right)}\left(\frac{\sigma_{\mathrm{AM}}}{5\ \text{Å}}\right)^2 \Omega_{\mathrm{AM}}^{2,2} \qquad (8)$$

where $\Omega_{\mathrm{AM}}^{2,2}$ is the collision integral, which is approximated by[32]

$$\Omega_{AM}^{2,2} \approx \left[0.697 + 0.5185 \log\left(\frac{kT}{\xi_{AM}}\right)\right] \quad (9)$$

In these expressions μ_{AM} is the reduced mass of the adduct and the collision partner, σ_{AM} is the Lennard-Jones collision diameter given by $(\sigma_A + \sigma_M)/2$, and ξ_{AM} is the Lennard-Jones well depth given by $(\xi_{AA}\xi_{MM})^{0.5}$. For these calculations, the collision partner was assumed to be nitrogen, with $\sigma = 3.8$ Å and $\xi/k = 71.4$ K. The Lennard-Jones parameters for the adducts ($\sigma = 5.3$ Å and $\xi/k = 384$ K) were estimated using the method of Chung et al.[35,36] based on the critical temperature and volume for isoprene.[36]

The density of states at the critical energy, $\rho(E_0)$, was calculated using the Whitten−Rabinovitch approximation,[37,38] and the vibrational partition function (Q_{vib}) for each adduct was calculated using the B3LYP/6-31G** vibrational frequencies (Table 2). The correction terms F_E, F_{anh}, and F_{rot} were calculated following Troe[32,33] and Patrick and Golden.[34] The equilibrium constant K_{eq} for the reaction was calculated based on spectroscopic data derived from the MP2/6-311G** optimized geometries and B3LYP/6-31G** frequencies for the adducts and the OH + isoprene reactants. The weak-collision association rate constant, k_{rec}^{wc} was obtained by multiplying the strong-collision association rate constant, k_{rec}^{sc} (from eq 7), by a collisional deactivation efficiency, β_c, which is derived by comparison with experiment.[34]

The values for each parameter in eq 6 were calculated for each adduct in order to compare the calculated $k_{rec,0}^{wc}$ with recent experimental measurements of the pressure dependence of the OH + isoprene reaction.[39] These experimental results indicate that the OH + isoprene reaction does not display low-pressure limiting behavior at temperatures below 343 K. As a result, the low-pressure limiting rate constant was calculated from 343 to 423 K, where the OH + isoprene reaction displays falloff behavior at pressures between 2 and 6 Torr. The detailed results for each adduct are summarized in Tables 4−7, and the overall results for all four adducts are summarized in Table 8. In these tables, the individual parameters are calculated using the calculated stabilization energy for each adduct at the PMP4/6-311G**//MP2/6-311G** + ΔZPE level of theory (Table 3).

As can be seen from Table 8, the predicted values for the overall termolecular rate constant for the OH + isoprene reaction, which is the sum of the rate constant for formation of each adduct, are in reasonable agreement with the experimental values over this temperature range when the calculated stabilization energies of each adduct are used for the critical energy with a collisional deactivation efficiency of 0.0005. This empirically derived collisional deactivation efficiency is smaller than typical values of 0.1−0.5, and is probably due to incorrectly assuming that F_{corr}, the correction factor to account for coupling between the various degrees of freedom, is equal to unity.[34] As discussed above, the calculation of the vibrational frequencies shows that these modes for the OH−isoprene adducts are highly coupled to each other. If a typical collisional deactivation efficiency (β_c) of 0.1 is used in this calculation, a stabilization energy of approximately 29 kcal/mol for adducts 1 and 4 and 15 kcal/mol for adducts 2 and 3 for the critical energy E_0 is required to bring the calculated termolecular rate constants into agreement with experiment. The results of these calculations suggest that the theoretical stabilization energies of the adducts are in reasonable agreement with experiment to within 10 kcal/mol. This is a conservative estimate of the error associated with the ab initio calculations.

At the low-pressure limit of the reaction, the reactivity of the OH + isoprene system is dominated by the formation of the more stable adducts 1 and 4, as the lower stability of adducts 2 and 3 lead to much larger dissociation rate constants, and therefore smaller association rate constants. As a result, the overall yield of each adduct at the low-pressure limit is predicted to be approximately 72% for adduct 1 and 28% for adduct 4, with adducts 2 and 3 contributing less than 1% to the overall yield. Assuming that these results also reflect the adduct yield at atmospheric pressure and that addition favors the radical that is the most stable, the calculated stabilities are consistent with the measured product yields for this reaction,[19] as adducts 1 and 4 lead to the production of methyl vinyl ketone and methacrolein in the OH-initiated oxidation of isoprene (reaction paths a and e in Figure 1). The higher stability of adducts 1 and 4 also suggests the potential for significant carbonyl production through reaction paths b and f in Figure 1, which is consistent with experimental observations.[17,18]

Our calculated results are consistent with the assumed yields of 59%, 5%, 5%, and 31% for adducts 1−4 used in the model of Jenkin et al. based on structure−reactivity relationships.[4] These results are also consistent with experimental studies of the OH + methyl vinyl ketone reaction, which suggests that OH preferentially adds to the terminal carbon (adducts 1 and 4 for isoprene).[5] However, these results are in contrast to the preferential reactivity predictions for the OH + isoprene reaction based on empirical evidence from OH + diolefins reactions,[3] which predicts that OH should preferentially add to the trisubstituted double bond (adducts 1 and 2) over the unsubstituted double bond (adducts 3 and 4).[1] On the basis of this, Paulson and Seinfeld assumed yields of 35%, 24%, 16% and 24% for adducts 1−4, respectively, in their mechanism of the OH-initiated oxidation of isoprene.[1]

However, the calculated results at low pressure may not be applicable to the overall yield of each adduct under atmospheric conditions. At the high-pressure limit, the association rate constant is no longer limited by intermolecular energy transfer, but instead is limited by intramolecular processes.[31] As a result, the rate constant and adduct yield for the OH + isoprene reaction will depend on the structures and energetics of the transition states leading to formation of each adduct, rather than the relative stability of the adduct. Given that the barrier to formation of the adducts is probably negligible, it is possible that the overall rates of formation of each adduct are similar, as the differences between the structure and energetics of the individual transition states may be negligible, similar to that found for the transition states of the OH + propene reaction.[23]

As a result, although these theoretical calculations are generally consistent with present assumptions of the product yields of the OH addition to isoprene, they do not rule out the possibility that adducts 2 and 3 can contribute significantly to the formation of methyl vinyl ketone, methacrolein, and other oxidation products through reaction paths c and d in Figure 1.[18] Assuming that the overall rate of formation of each adduct is approximately equal, the ability of adducts 2 and 3 to contribute to the product distribution of the OH-initiated oxidation of isoprene depends on the unimolecular dissociation lifetime of each adduct relative to reaction with O_2 under atmospheric conditions. The unimolecular dissociation lifetime of each adduct was estimated using the equilibrium constants calculated as above at 300 K, and the measured rate constant for the OH + isoprene reaction at the high-pressure limit and 300 K (overall rate at 1×10^{-10} cm^3 molecule^{-1} s^{-1}).[7,39] Assuming that the barrier to formation of each individual adduct is negligible and that all four adducts contribute equally to the overall forward rate constant at the high-pressure limit, this calculation results

TABLE 4: Contributing Factors to the Calculation of the Strong Collision Dissociation and Recombination Rate Constants for the OH + Isoprene → Adduct 1 Reaction Using the ab Initio Calculated Stabilization Energy of −37.9 kcal mol^{-1}

T (K)	Z_{LJ} (cm^{3}mol^{-1}s^{-1})	$\rho(E_0)$	Q_{vib}	F_E; F_{anh}; F_{rot}	k_{diss}^{sc} (cm^3 mol^{-1} s^{-1})	K_{eq} (mol cm^{-3})	k_{rec}^{sc} (cm^6 mol^{-2} s^{-1})
343	4.4×10^{-10}	8.7×10^{9}	118.7	1.3; 1.1; 5.6	5.2×10^{-22}	3.7×10^{1}	1.4×10^{-23}
363	4.5×10^{-10}		166.9	1.4; 1.1; 5.2	8.1×10^{-21}	8.2×10^{2}	1.0×10^{-23}
383	4.6×10^{-10}		235.1	1.4; 1.1; 4.9	9.2×10^{-20}	1.3×10^{4}	7.1×10^{-24}
403	4.6×10^{-10}		331.3	1.4; 1.1; 4.6	7.9×10^{-19}	1.6×10^{5}	5.0×10^{-24}
423	4.7×10^{-10}		467.3	1.4; 1.1; 4.3	5.3×10^{-18}	1.5×10^{6}	3.6×10^{-24}

TABLE 5: Contributing Factors to the Calculation of the Strong Collision Dissociation and Recombination Rate Constants for the OH + Isoprene → Adduct 2 Reaction Using the ab Initio Calculated Stabilization Energy of −25.6 kcal mol^{-1}

T (K)	Z_{LJ} (cm^{3}mol^{-1} s^{-1})	$\rho(E_0)$	Q_{vib}	F_E; F_{anh}; F_{rot}	k_{diss}^{sc} (cm^3 mol^{-1} s^{-1})	K_{eq} (mol cm^{-3})	k_{rec}^{sc} (cm^6 mol^{-2} s^{-1})
343	4.4×10^{-10}	2.5×10^{7}	73.8	1.4; 1.1; 4.6	1.4×10^{-16}	4.9×10^{9}	2.9×10^{-26}
363	4.5×10^{-10}		105.9	1.5; 1.1; 4.1	8.0×10^{-16}	3.9×10^{10}	2.0×10^{-26}
383	4.6×10^{-10}		152.3	1.5; 1.1; 3.9	3.6×10^{-15}	2.5×10^{11}	1.4×10^{-26}
403	4.6×10^{-10}		219.3	1.5; 1.1; 3.6	1.4×10^{-14}	1.3×10^{12}	1.0×10^{-26}
423	4.7×10^{-10}		316.1	1.6; 1.1; 3.4	4.4×10^{-14}	6.0×10^{12}	7.4×10^{-27}

TABLE 6: Contributing Factors to the Calculation of the Strong Collision Dissociation and Recombination Rate Constants for the OH + Isoprene → Adduct 3 Reaction Using the Ab Initio Calculated Stabilization Energy of −24.2 kcal mol^{-1}

T (K)	Z_{LJ} (cm^{3}mol^{-1} s^{-1})	$\rho(E_0)$	Q_{vib}	F_E; F_{anh}; F_{rot}	k_{diss}^{sc} (cm^3 mol^{-1} s^{-1})	K_{eq} (mol cm^{-3})	k_{rec}^{sc} (cm^6 mol^{-2} s^{-1})
343	4.4×10^{-10}	2.7×10^{7}	166.6	1.4; 1.1; 4.4	5.2×10^{-16}	1.6×10^{10}	3.3×10^{-26}
363	4.5×10^{-10}		241.5	1.5; 1.1; 4.1	2.6×10^{-15}	1.1×10^{11}	2.3×10^{-26}
383	4.6×10^{-10}		350.2	1.5; 1.1; 3.8	1.1×10^{-14}	6.4×10^{11}	1.6×10^{-26}
403	4.6×10^{-10}		507.9	1.5; 1.1; 3.6	3.6×10^{-14}	3.1×10^{12}	1.2×10^{-26}
423	4.7×10^{-10}		736.8	1.6; 1.1; 3.4	1.1×10^{-13}	2.3×10^{13}	8.5×10^{-27}

TABLE 7: Contributing Factors to the Calculation of the Strong Collision Dissociation and Recombination Rate Constants for the OH + Isoprene → Adduct 4 Reaction Using the ab Initio Calculated Stabilization Energy of −35.4 kcal mol^{-1}

T (K)	Z_{LJ} (cm^{3}mol^{-1} s^{-1})	$\rho(E_0)$	Q_{vib}	F_E; F_{anh}; F_{rot}	k_{diss}^{sc} (cm^3 mol^{-1} s^{-1})	K_{eq} (mol cm^{-3})	k_{rec}^{sc} (cm^6 mol^{-2} s^{-1})
343	4.4×10^{-10}	3.2×10^{9}	125.2	1.3; 1.1; 5.4	6.9×10^{-21}	1.3×10^{3}	5.4×10^{-24}
363	4.5×10^{-10}		175.9	1.4; 1.1; 5.0	8.7×10^{-20}	2.3×10^{4}	3.8×10^{-24}
383	4.6×10^{-10}		247.7	1.4; 1.1; 4.7	8.2×10^{-19}	3.1×10^{5}	2.7×10^{-24}
403	4.6×10^{-10}		349.1	1.4; 1.1; 4.4	6.0×10^{-18}	3.1×10^{6}	1.9×10^{-24}
423	4.7×10^{-10}		492.5	1.4; 1.1; 4.2	3.5×10^{-17}	2.6×10^{7}	1.4×10^{-24}

TABLE 8: Calculated Overall Recombination Rate Constants for the OH + Isoprene Reaction Using ab Initio Stabilization Energies

T (K)	k_{rec}^{wc}(ab initio) ($\beta = 0.0005$) (cm^6 mol^{-2} s^{-1})	k_{exp}[a] (cm^6 mol^{-2} s^{-1})
343	9.7×10^{-27}	1.1×10^{-26}
363	6.9×10^{-27}	6.7×10^{-27}
383	4.9×10^{-27}	5.4×10^{-27}
403	3.5×10^{-27}	4.5×10^{-27}
423	2.5×10^{-27}	3.7×10^{-27}

[a] Experimental values from ref 39.

in estimated unimolecular dissociation lifetimes of approximately 3×10^{12} and 6×10^{10} s at 300 K for adducts 1 and 4, respectively, and 1800 and 400 s at 300 K for adducts 2 and 3, respectively, using the ab initio calculated stabilization energies ($K_{eq} = 1.2 \times 10^{-2}$, 2.2×10^{7}, 9.6×10^{7}, 6.9×10^{-1} cm^{-3} for adducts 1−4, respectively). These lifetimes are considerably longer than the collisional lifetime of each adduct with O_2 under tropospheric conditions (approximately 1×10^{-7} s), suggesting that the stability of all four adducts allows each to participate in subsequent steps in the OH-initiated oxidation of isoprene. As a result, the overall yield of adducts 2 and 3 at atmospheric pressure and their contribution to the overall mechanism of isoprene oxidation may be greater than that predicted at the low-pressure limit.

Experimental Detection of the OH + Isoprene Adducts. To verify the predicted yields of the OH−isoprene adducts, the products of the OH + isoprene reaction were measured and identified at a pressure of 1−10 Torr using the DF/MS technique. It has been shown experimentally that the OH + isoprene reaction has reached its high-pressure limit in this pressure regime;[7,39] thus these experiments should be applicable to atmospheric conditions for this reaction. Approximately 9×10^{12} cm^{-3} of OH radicals were added through a movable injector and reacted with approximately 2.2×10^{13} cm^{-3} of isoprene added to the reactor through a side-arm port. The reaction time was adjusted by moving the position of the movable injector so that the OH radicals were completely titrated, reducing the observed isoprene signal at $m/e = 68$ by nearly a factor of 2. With the mass spectrometer operating at 40 eV of electron impact energy and 3 mA of emission current, strong signals due to the products of the OH + isoprene reaction were observed at $m/e = 85$, 71, 58, 54, 43, 41, 31, and 14. These signals were confirmed to be due to the products of the OH + isoprene reaction, as the intensity of each signal decreased when the microwave discharge, the F_2, or the H_2O was turned off. The signal at m/e 85 corresponds to the parent ion of the HO−isoprene adduct, while the remaining signals were assigned to daughter peaks due to fragmentation of each of the individual adducts and unreacted isoprene.

The signals at $m/e = 71$ and $m/e = 14$ correspond to the daughter fragments resulting from either breaking the C_3-C_4 bond in adduct 3 or the C_1-C_2 bond in adduct 2. The signal at $m/e = 58$ corresponds to the daughter fragment resulting from

cleavage at the C_2-C_3 bond in adduct 1 or adduct 2. The signals at $m/e = 54$ and $m/e = 31$ correspond to the fragment resulting from breaking the C_1-C_2 bond in adduct 1 or the C_3-C_4 bond in adduct 4, while the signals at $m/e = 43$ and $m/e = 41$ correspond to breaking the C_2-C_3 bond in adducts 3 or 4. Residual signals at $m/e = 54$, 41, and 14 after the microwave discharge was turned off correspond to daughter fragments resulting from the breaking of the C_2-C_3 bond and the C_3-C_4 bond of isoprene.

The fragmentation signal at $m/e = 71$ is unique to adducts 2 and 3, while the signal at $m/e = 31$ is unique to adducts 1 and 4. Thus, although these experiments do not provide any quantitative data on the relative yield of each adduct, there is evidence for the formation of all four adducts under these experimental conditions, suggesting that the rates of formation of adducts 2 and 3 are nonnegligible at the high-pressure limit of the reaction. This implies that although the theoretical results suggest that adducts 1 and 4 should be the dominant products formed from the OH + isoprene reaction due to their higher stability and longer lifetimes, the rates of formation of each adduct are not limited by intermolecular energy transfer, and thus are not dependent on the relative stabilization energy of each adduct. Instead, the rates of formation of each adduct are limited by intramolecular processes that are dependent on the structure and energies of the individual transition states. Since it is likely that there is no energy barrier for the addition of OH to isoprene, the differences between the structure and energetics of the individual transition states may be negligible. As a result, the formation of each adduct will probably be determined statistically by the collision between the OH radical and the skeleton carbon atom of the isoprene molecule, resulting in an approximately equal distribution of all four adducts. The experimental results also indicate that the unimolecular lifetimes of each adduct are longer than the 60−160 ms residence time in these experiments, and suggest that the stability of all four adducts allows each to participate in subsequent steps in the OH-initiated oxidation of isoprene. As a result, the overall product yields for the OH-initiated oxidation of isoprene will likely be determined by the subsequent reactivity of these adducts, rather than a preferential formation of the individual adducts. However, calculations of the properties of the individual transition states for the formation of each adduct are needed to confirm these results.

Summary

Ab initio calculations on the products of the OH + isoprene reaction reveal that the addition of OH to the terminal carbons leads to the formation of products that are more energetically stable than the products formed through addition to the internal carbons. At the PMP4(STDQ)/6-311G**//MP2/6-311G** + ΔZPE level of theory, the adducts resulting from the addition of OH to the 1 and 4 carbons of isoprene are 37.9 and 35.4 kcal mol^{-1} more stable than the OH and isoprene reactants, while the adducts produced from OH addition to the 2 and 3 carbons have a relative stability of 25.6 and 24.2 kcal mol^{-1}, respectively. The higher stability of the 1 and 4 adducts resulting from addition to the terminal carbons of isoprene is likely due to the ability of these adducts to delocalize the unpaired electron resulting from the OH radical addition due to the allylic nature of these adducts. These results are in contrast to preferential reactivity predictions for the OH + isoprene reaction based on empirical evidence from OH + diolefins reactions.[1,3] These stabilization energies result in estimated termolecular rate constants for the OH + isoprene reaction using simplified calculations based on RRKM theory that are in reasonable agreement with experiment values between 343 and 423 K.

Although these theoretical results suggest that the adducts resulting from addition of OH to the terminal carbons of isoprene should dominate the product distribution for this reaction, consistent with the observed product distribution for the OH-initiated oxidation of isoprene under high NO_x conditions, measurements of the products of the OH + isoprene reaction using DF/MS techniques show evidence for the production of all four adducts. These experimental results suggest that each adduct is formed with nonnegligible yields at the high-pressure limit of the OH + isoprene reaction. These results also suggest that the stability of each adduct relative to the reactants results in unimolecular dissociation lifetimes that are long enough for each adduct to participate in subsequent steps in the OH-initiated oxidation of isoprene. These experimental results are consistent with the calculated stability of all four OH−isoprene adducts and may imply that the high stability of all four adducts leads to a product distribution for the OH + isoprene → adduct reaction at the high-pressure limit that may be statistically based rather than determined by the relative energetics of the individual adducts. Further calculations of the properties of the transition states for the OH + isoprene reaction are needed to confirm these results.

Acknowledgment. This work is supported in part by grants from the National Science Foundation to Indiana University (ATM-9622712) and to the University of Illinois (ATM-9813331), and by a grant from the U.S. Environmental Protection Agency (x8255967-01-0 EPA) to the University of Illinois. Acknowledgment is also made to the donors of the Petroleum Research Fund, administered by the American Chemical Society, for partial support of this research (PRF 33643-G6 to Indiana University). Z.L. thanks NCSA for supercomputer time to support this work. We also acknowledge helpful discussions with J. Abbatt, and the critical and constructive comments of the reviewers.

References and Notes

(1) Paulson, S. E.; Seinfeld, J. H. *J. Geophys. Res.* **1992**, *97*, 20703.
(2) Seinfeld, J. H.; Pandis, S. N. *Atmospheric Chemistry and Physics: From Air Pollution to Climate Change*; John Wiley and Sons: New York, 1998.
(3) Ohta, T. *J. Phys. Chem.* **1983**, *87*, 1209.
(4) Jenkin, M. E.; Boyd, A. A.; Lesclaux, R. *J. Atmos. Chem.* **1998**, *29*, 267.
(5) Tuazon, E. C.; Atkinson, R. *Int. J. Chem. Kinet.* **1989**, *21*, 1141.
(6) Kleindienst, T. E.; Harris, G. W.; Pitts, J. N. Jr. *Environ. Sci. Technol.* **1982**, *16*, 844.
(7) Stevens, P.; L′Esperance, D.; Chuong, B.; Martin, G. *Int. J. Chem. Kinet.* **1999**, *31*, 637.
(8) Atkinson, R. *J. Phys. Chem. Ref. Data* **1997**, *26* (6), 1329.
(9) Atkinson, R.; Aschmann, S. M.; Winer, A. M.; Pitts, J. N. Jr. *Int. J. Chem. Kinet.* **1982**, *14*, 507.
(10) Atkinson, R.; Aschmann, S. M. *Int. J. Chem. Kinet.* **1984**, *16*, 1175.
(11) Gu, C.; Rynard, C. M.; Hendry, D. G.; Mill, T. *Environ. Sci. Technol.* **1985**, *19*, 151.
(12) Tuazon, E. C.; Atkinson, R. *Int. J. Chem. Kinet.* **1990**, *22*, 1221.
(13) Paulson, S. E.; Flagan, R. C.; Seinfeld, J. H. *Int. J. Chem. Kinet.* **1992**, *24*, 79.
(14) Atkinson, R.; Aschmann, S. M.; Tuazon, E. C.; Arey, J.; Zielinska, B. *Int. J. Chem. Kinet.* **1989**, *21*, 593.
(15) Grosjean, D.; Williams, E. L. II; Grosjean, E. *Environ. Sci. Technol.* **1993**, *27*, 830.
(16) Miyoshi, A.; Hatakeyama, S.; Washida, N. *J. Geophys. Res.* **1994**, *99*, 18799.
(17) Kwok, E. C.; Atkinson, R.; Arey, J. *Environ. Sci. Technol.* **1995**, *29*, 2467.
(18) Yu, J.; Jeffries, H. E.; Le Lacheur, R. M. *Environ. Sci. Technol.* **1995**, *29*, 1923.
(19) Carter, W. P. L.; Atkinson, R. *Int. J. Chem. Kinet.* **1996**, *28*, 497.

(20) Chen, X.; Hulbert, D.; Shepson, P. B. *J. Geophys. Res.* **1998**, *103*, 25563.

(21) McKeen, S. A.; Mount, G.; Eisele, F.; Williams, E.; Harder, J.; Goldan, P.; Kuster, W.; Liu, S. C.; Baumann, K.; Tanner, D.; Fried, A.; Sewell, S.; Cantrell, C.; Shetter, R. *J. Geophys. Res.* **1997**, *102*, 6467.

(22) Sosa, C.; Schlegel, H. B. Sosa, C. *J. Am. Chem. Soc.* **1986**, *109*, 7007. Schlegel, H. B. *J. Am. Chem. Soc.* **1987**, *109*, 4193. Smith, B.; Nguyen, M. T.; Bouma, W. J.; Radom, L. *J. Am. Chem. Soc.* **1991**, *113*, 6452. Villa, J.; Gonzalez-Lafont, A.; Lluch, J. M.; Corchado, J. C.; Espinosa-Garcia, J. *J. Phys. Chem.* **1997**, *107*, 77266.

(23) Díaz-Acosta, I.; Alvarez-Idaboy, J. R.; Vivier-Bunge, A. *Int. J. Chem. Kinet.* **1999**, *31*, 29.

(24) HyperChem Release 5.0, Hypercube Inc., Ontario, Canada, 1996.

(25) Frisch, M. J.; Trucks, G. W.; Schlegel, H. B.; Scuseria, G. E.; Robb, M. A.; Cheeseman, J. R.; Zakrzewski, V. G.; Montgomery, J. A.; Stratmann, R. E.; Burant, J. C.; Dapprich, S.; Millam, J. M.; Daniels, A. D.; Kudin, K. N.; Strain, M. C.; Farkas, O.; Tomasi, J.; Barone, V.; Cossi, M.; Cammi, R.; Mennucci, B.; Pomelli, C.; Adamo, C.; Clifford, S.; Ochterski, J.; Petersson, G. A.; Ayala, P. Y.; Cui, Q.; Morokuma, K.; Malick, D. K.; Rabuck, A. D.; Raghavachari, K.; Foresman, J. B.; Cioslowski, J.; Ortiz, J. V.; Stefanov, B. B.; Liu, G.; Liashenko, A.; Piskorz, P.; Komaromi, I.; Gomperts, R.; Martin, R. L.; Fox, D. J.; Keith, T.; Al-Laham, M. A.; Peng, C. Y.; Nanayakkara, A.; Gonzalez, C.; Challacombe, M.; Gill, P. M. W.; Johnson, B. G.; Chen, W.; Wong, M. W.; Andres, J. L.; Head-Gordon, M.; Replogle, E. S.; Pople, J. A. *Gaussian 98*; Gaussian, Inc.: Pittsburgh, PA, 1998.

(26) Li, Z. *J. Phys. Chem. A* **1999**, *103*, 1206.

(27) Traetteberg, M.; Paulen, G.; Cyvin, S. J.; Panchenko, Y. N.; Mochalov, V. I. *J. Mol. Struct.* **1984**, *116*, 141.

(28) *JANAF Thermochemical Tables*, 3rd ed.; Chase, M. W. Jr., Davies, C. A., Downey, J. R., Frurip, D. J., McDonald, R. A., Syverud, A. N., Eds.; National Standards Reference Data Series, Vol. 14; National Bureau of Standards: Washington, DC, 1985.

(29) Herzberg, G. *Molecular Spectra and Molecular Structure II*; Krieger: Malabar, FL, 1988; p 335.

(30) Becke, A. D. *J. Chem. Phys.* **1993**, *98*, 5648.

(31) Troe, J. *J. Chem. Phys.* **1977**, *66*, 4745.

(32) Troe, J. *J. Chem. Phys.* **1977**, *66*, 4758.

(33) Troe, J. *J. Phys. Chem.* **1979**, *83*, 114.

(34) Patrick, R.; Golden, D. M. *Int. J. Chem. Kinet.* **1983**, *15*, 1189.

(35) Chung, T. H.; Lee, L. L.; Starling, K. E. *Ind. Eng. Chem. Fundam.* **1984**, *23*, 8.

(36) Reid, R. C.; Prausnitz, J. M.; Poling, B. E. *The Properties of Gases and Liquids*, 4th ed.; McGraw-Hill: New York, 1987.

(37) Whitten, G. Z.; Rabinovitch, B. S. *J. Chem. Phys.* **1963**, *38*, 2466; **1964**, *41*, 1883.

(38) Smith, I. W. M. *Kinetics and Dynamics of Elementary Gas Reactions*; Butterworths: London, 1980.

(39) Chuong, B.; Stevens, P. S. *J. Phys. Chem. A*, in press.